lc-review

DATASET · OCTOBER 2014

DOI: 10.13140/2.1.1238.3686

2 AUTHORS, INCLUDING:

Takao Tsuneda

University of Yamanashi

68 PUBLICATIONS **3,903** CITATIONS

Advanced Review

Long-range correction for density functional theory

Takao Tsuneda[1]* and Kimihiko Hirao[2]

Long-range correction for exchange functionals in Kohn–Sham density functional theory and its applicability are reviewed. Long-range correction simply supplements the long-range exchange effect in exchange functionals by replacing the Hartree–Fock exchange integral with the long-range part of exchange functionals. Nevertheless, this correction has solved many problems in Kohn–Sham calculations. Using this correction, valence occupied and unoccupied orbital energies are quantitatively reproduced in a comprehensive manner for the first time. Long-range correction has also solved the underestimations of charge transfer excitation energies and oscillator strengths in time-dependent Kohn–Sham calculations and has clearly improved poor optical response properties such as hyperpolarizability in coupled-perturbed Kohn–Sham and finite-field calculations. Moreover, this correction has drastically improved the reproducibility of van der Waals bonds by simply combining with conventional van der Waals calculation methods. We, therefore, believe that the long-range correction clearly extends the applicability of the Kohn–Sham method in future quantum chemistry calculations.

How to cite this article:
WIREs Comput Mol Sci 2014, 4:375–390. doi: 10.1002/wcms.1178

LONG-RANGE CORRECTION

Formulation of Long-Range Correction

Long-range correction (LC) in density functional theory (DFT) indicates the correction of exchange functionals for long-range electron–electron exchange interactions, which are insufficiently incorporated in conventional exchange functionals. Since these functionals usually depend only on the electron distribution, they essentially contain no explicit electron–electron interaction. Exchange functionals are generally represented in the form of a one-electron coordinate integral,

$$E_x^{\mathrm{DF}} = -\frac{1}{2}\sum_{\sigma}\int d^3\mathbf{r}\rho_\sigma^{4/3}(\mathbf{r})K_\sigma[x_\sigma(\mathbf{r})], \tag{1}$$

where $\mathbf{r}$ is the coordinate vector of electrons, ρ_σ is the σ-spin electron density, and K_σ is a dimensionless factor, which is usually a functional of the dimensionless parameter, $x_\sigma = |\nabla\rho_\sigma|/\rho_\sigma^{4/3}$ in pure generalized gradient approximation (GGA) exchange functionals. Therefore, it is clear that these exchange functionals contain no long-range exchange interaction. In contrast, long-range exchange interactions are naturally incorporated in the Hartree–Fock (HF) exchange integral, which is an explicit two-electron integral:

$$E_{\mathrm{x}}^{\mathrm{HF}} = -\frac{1}{2}\sum_{\sigma}\sum_{i}\sum_{j}\iint d^3\mathbf{r}_1 d^3\mathbf{r}_2\phi_{i\sigma}^*(\mathbf{r}_1)\phi_{j\sigma}(\mathbf{r}_1) \times \frac{1}{r_{12}}\phi_{i\sigma}(\mathbf{r}_2)\phi_{j\sigma}^*(\mathbf{r}_2), \tag{2}$$

where $\phi_{i\sigma}$ is the ith σ-spin orbital and r_{12} is the electron–electron distance, $r_{12} = |\mathbf{r}_2 - \mathbf{r}_1|$. We and our co-workers developed long-range correction, in which exchange interactions are partitioned into short- and long-range parts and then a general exchange functional and the HF exchange integral are adopted in the calculations of the short- and long-range parts, respectively.[1] For the local density

The authors have declared no conflicts of interest in relation to this article.

*Correspondence to: ttsuneda@yamanashi.ac.jp

[1]Fuel Cell Nanomaterials Center, University of Yamanashi, Kofu, Japan

[2]Computational Chemistry Unit, RIKEN Advanced Institute for Computational Science, Kobe, Hyogo, Japan

DOI: 10.1002/wcms.1178

approximation (LDA) exchange functional,[2] Savin suggested formulating the LC scheme,[3] which is now called the "range-separation hybrid (RSH) exchange functional," by combining the long-range corrected exchange functionals with short-range correlation functionals. Long-range correction makes it applicable to general functionals, making it useful in quantum chemistry calculations. In this correction, the two-electron operator, $1/r_{12}$, is partitioned by the standard error function as

$$\frac{1}{r_{12}} = \frac{1-\mathrm{erf}(\mu r_{12})}{r_{12}} + \frac{\mathrm{erf}(\mu r_{12})}{r_{12}}, \tag{3}$$

where μ is a parameter for determining the division ratio. However, it is usually hard to divide exchange functionals by using Eq. (3) because conventional functionals have not been derived from the corresponding density matrix in general. In long-range correction, it is therefore assumed that all of the features of exchange functionals are reflected by the Fermi momentum k_σ for the LDA exchange functional. On this assumption, the short-range part of general exchange functionals in Eq. (1) is derived as

$$E_{\mathrm{x}}^{\mathrm{LC(sr)}} = -\frac{1}{2}\sum_\sigma \int d^3\mathbf{r}\rho_\sigma^{4/3} K_\sigma \left\{1 - \frac{8}{3}a_\sigma \times \left[\sqrt{\pi}\,\mathrm{erf}\left(\frac{1}{2a_\sigma}\right) + 2a_\sigma\,(b_\sigma - c_\sigma)\right]\right\}, \tag{4}$$

where a_σ, b_σ, and c_σ are given as

$$a_\sigma = \frac{\mu}{2k_\sigma} = \frac{\mu K_\sigma^{1/2}}{6\sqrt{\pi}\,\rho_\sigma^{1/3}}, \tag{5}$$

$$b_\sigma = \exp\left(-\frac{1}{4a_\sigma^2}\right) - 1, \tag{6}$$

and

$$c_\sigma = 2a_\sigma^2 b_\sigma + \tfrac{1}{2}. \tag{7}$$

Note that in Eq. (5), k_σ is derived to provide the Fermi momentum, $k_{\mathrm{F}\sigma} = (6\pi^2\rho_\sigma)^{1/3}$, for the LDA exchange functional, $K_\sigma^{\mathrm{LDA}} = 3\,(3/4\pi)^{1/3}$, as

$$k_\sigma = \left(\frac{9\pi}{K_\sigma}\right)^{1/2}\rho_\sigma^{1/3}. \tag{8}$$

Using this momentum, Eq. (4) becomes identical to the previously proposed long-range correction for the LDA exchange functional.[3] The long-range part of the HF exchange integral is simply given by multiplying the standard error function by the two-electron operator in Eq. (2) as

$$E_{\mathrm{x}}^{\mathrm{LC(lr)}} = -\frac{1}{2}\sum_\sigma\sum_i^n\sum_j^n \iint d^3\mathbf{r}_1 d^3\mathbf{r}_2 \phi_{i\sigma}^*(\mathbf{r}_1)\phi_{j\sigma}(\mathbf{r}_1) \times \frac{\mathrm{erf}\,(\mu r_{12})}{r_{12}}\phi_{i\sigma}(\mathbf{r}_2)\phi_{j\sigma}^*(\mathbf{r}_2). \tag{9}$$

Naturally, the only parameter, μ, depends on the corrected exchange functional: for example, the μ value of the B88 and Perdew–Burke–Ernzerhof (PBE) exchange functionals is optimized as $\mu = 0.47$ for electronic ground states at around equilibrium geometries[4] and as $\mu = 0.33$ for other properties including response properties.[1]

Despite its simple correction style of using only one parameter, it has been proven that this correction solves an astonishing variety of problems occurring in Kohn–Sham calculations. The availability of long-range correction is reviewed in the section *DFT Problems That Long-Range Correction Has Solved*.

Long-Range Corrected Functionals

Besides the original functionals, various long-range corrected functionals have been developed due to the high applicability of long-range correction. Let us briefly introduce the formulations, advantages, and disadvantages of major long-range corrected functionals in this section.

The CAM-B3LYP functional[5] is a long-range corrected hybrid functional that uses

$$\frac{1}{r_{12}} = \frac{1-[\alpha+\beta\cdot\mathrm{erf}(\mu r_{12})]}{r_{12}} + \frac{\alpha+\beta\cdot\mathrm{erf}(\mu r_{12})}{r_{12}}, \tag{10}$$

as a substitute for Eq. (3) to perform long-range correction for the B3LYP hybrid functional.[6] Although several values of α and β have been used, $\alpha = 0.19$ and $\beta = 0.46$ seem to be the most common. The main feature of this functional is the inclusion of the short-range HF exchange integral at a constant rate instead of the incomplete long-range exchange integral. For the correlation functional, the sum of 0.19 times the Vosko–Wilk–Nusair LDA functional and 0.81 times the Lee–Yang–Parr (LYP) GGA functional[7] are used similarly to the B3LYP functional. The CAM-B3LYP functional was developed on the basis of the concept that the poor atomization energies of the original long-range corrected functionals are attributable to the uncorrected short-range exchange functional, the atomization energies being reported as the most critical problem in the benchmark set calculations. As a result, atomization energies are clearly improved,

while maintaining the accuracy of other properties in the benchmark set calculations.

Contrasting with the momentum transformation of the original long-range correction in Eq. (8), the LC-ωPBE functional[8] is derived by using the corresponding exchange hole of the PBE exchange functional[9] as

$$E_{\mathrm{x}}^{\mathrm{LC}\text{-}\omega\mathrm{PBE(sr)}}(\omega) = 2\pi \int d^3\mathbf{r}\rho(\mathbf{r}) \int_0^\infty \mathrm{d}r_{12}[1 - \mathrm{erf}(\omega r_{12})] \times r_{12} h_{\mathrm{x}}^{\mathrm{PBE}}(\mathbf{r}, r_{12}), \quad (11)$$

where ω, which is identical to the μ parameter of the original one, is given as $\omega = 0.4$. The advantage of this functional comes down to the high physical validity of the short-range exchange part.

Long-range correction is also applied to a semiempirical functional. The first long-range corrected semiempirical functional is the ωB97X functional[10] in the form,

$$E_{\mathrm{xc}}^{\omega\mathrm{B97X}} = E_{\mathrm{x}}^{\mathrm{LC(lr)}} + c_{\mathrm{x}} E_{\mathrm{x}}^{\mathrm{HF(sr)}} + E_{\mathrm{x}}^{\mathrm{B97(sr)}} + E_{\mathrm{c}}^{\mathrm{B97}}, \quad (12)$$

where B97 indicates the B97 semiempirical functional.[11] For $c_{\mathrm{x}} = 0$, it is simply called the "ωB97" functional. This functional contains many semiempirical parameters: 17 parameters in ωB97X and 16 parameters in ωB97. Partly for that reason, it frequently gives more accurate results for properties including the atomization energies than do the original ones in benchmark set calculations. The ωB97XD functional is a van der Waals correction for the ωB97X functional in which a parameterized classical dispersion term is combined (see the section *Van der Waals Bonds*). Besides ωB97-series functionals, there are various long-range corrected semiempirical functional, for example, the LC-TPSS functional using the Tao–Perdew–Staroverov-Scuseria meta-GGA functional[12] for the short-range part.[13]

In the "LC-PR" functional,[14,15] the self-interaction correction is performed for the short-range exchange part of long-range corrected functionals. On the basis of the regional self-interaction correction,[16] the short-range exchange part is corrected by using the pseudospectral technique[17] such as

$$E_{\mathrm{x}}^{\mathrm{PR}} = \int d^3\mathbf{r} \left\{ [1 - f_{\mathrm{RS}}(t)]\, \epsilon_{\mathrm{x}}^{\mathrm{DF}} + f_{\mathrm{RS}}(t) \epsilon_{\mathrm{x}}^{\mathrm{SI}} \right\}, \quad (13)$$

$$\epsilon_{\mathrm{x}}^{\mathrm{SI}} = -\frac{1}{4} \sum_{\mu\nu\lambda\kappa} P_{\mu\nu} P_{\lambda\kappa} \chi_\nu^*(\mathbf{r}) \chi_\lambda(\mathbf{r}) \int d^3\mathbf{r}' \frac{\chi_\kappa^*(\mathbf{r}') \chi_\mu(\mathbf{r}')}{|\mathbf{r}' - \mathbf{r}|}, \quad (14)$$

and

$$f_{\mathrm{RS}}(t) = \begin{cases} 0 \ (t < a) \\ 1 \ (t \geq a) \end{cases} \quad (0 \leq a \leq 1), \quad (15)$$

where ϵ_x^{DF} is the exchange energy density defined by $E_x^{\mathrm{DF}} = \int d^3\mathbf{r}\epsilon_x^{\mathrm{DF}}$, χ_μ is the μth atomic orbital, and $P_{\mu\nu}$ is in element of the density matrix $\mathbf{P}$. The f_{RS} in Eq. (15) is a region-separation function for clipping the self-interaction region, where electrons exchange only with themselves, on the basis of $t = \tau^{\mathrm{W}}/\tau$ $(0 < t \leq 1)$, which is the ratio of the Weizsäcker kinetic energy density τ^{W} to the total one τ. This functional drastically improves the calculated core excitation energies of long-range corrected functionals in time-dependent Kohn–Sham (TDKS) calculations, while maintaining accuracy in core ionization energies, and valence, Rydberg, and charge transfer excitation energies (see the section *Electron Excitation Spectra*).[15] It is also reported that this functional provides accurate orbital energies simultaneously for core and valence orbitals (see the section *Valence Orbital Energies*).[14]

Various other long-range corrected functionals have so far been developed. The "erfgau" functional[18,19] mixes a Gaussian function term into the two-electron operator for improving the RSH functional, that is the long-range corrected LDA exchange functional. The "LCgau" functional[20] uses two modified parameters to increase the HF exchange integral in the short-range part:

$$\frac{1}{r_{12}} = \left[\frac{1 - \mathrm{erf}(\mu r_{12})}{r_{12}} - k \frac{2\mu}{\sqrt{\pi}} e^{-(1/a)\mu^2 r_{12}^2} \right] + \left[\frac{\mathrm{erf}(\mu r_{12})}{r_{12}} + k \frac{2\mu}{\sqrt{\pi}} e^{-(1/a)\mu^2 r_{12}^2} \right], \quad (16)$$

where k and a are set as 1 and 3 in the erfgau functional and -18.0 and 0.011 in the LCgau functional. On the basis of the adiabatic connection, which is the basic concept of hybrid functionals such as the B3LYP functional,[6] the Mori-Sanchez–Cohen–Yang (MCY) functional[21] is constructed as

$$E_{\mathrm{xc}}^{\mathrm{MCY}} = \int_0^1 d\lambda \left(W_\lambda^{\mathrm{DF}}[\rho] - W_\lambda^{\mathrm{LC(sr)}}[\rho] + W_\lambda^{\mathrm{LC(lr)}}[\rho] \right), \quad (17)$$

$$W_\lambda[\rho] = 2\lambda E_{\mathrm{xc}}\left[\rho_{1/\lambda}\right] + \lambda^2 \frac{dE_{\mathrm{xc}}\left[\rho_{1/\lambda}\right]}{d\lambda}, \quad (18)$$

where $\rho_{1/\lambda}(\mathbf{r}) = \rho(\mathbf{r}/\lambda)/\lambda^3$ and $\nabla\rho_{1/\lambda}(\mathbf{r}) = \nabla\rho(\mathbf{r}/\lambda)/\lambda^4$. In the Baer–Neuhauser–Livshitz functional,[22] the LYP GGA correlation functional is combined with the weakened RSH exchange functional, in which 0.9 times the short-range exchange term and $\mu = 0.5$ are used. The "M11"

functional[23] is a Mx-series meta semiempirical functional, in which the long-range correction is newly implemented. For use with Slater-type basis sets, long-range corrected functionals based on the Yukawa function, which is easily implemented in the integral calculation algorithm of this basis set, have been developed[24,25] as alternatives to the error function in Eq. (3). There may be other types of long-range corrected functionals. It is noteworthy that most of these functionals have common features, which are reviewed in the next section.

DFT PROBLEMS THAT LONG-RANGE CORRECTION HAS SOLVED

So far, long-range correction has solved various problems in Kohn–Sham density functional calculations. In this section, we discuss only the major properties by which the long-range correction makes it possible to perform quantitative calculations: valence orbital energies, electronic excitation spectra, response properties, and van der Waals bonds.

Valence Orbital Energies

Valence orbital energies may be the most significant property for which long-range correction enables quantitative calculations, because orbital energies, $\{\epsilon_i\}$, are just the solutions of the Kohn–Sham self-consistent field (SCF) equation,

$$\hat{F}\phi_i = \epsilon_i \phi_i, \tag{19}$$

where $\hat{F}$ is the Kohn–Sham Fock operator. Despite its significance, orbital energies had never been obtained quantitatively until recently. Most recently, only occupied orbital energies were accurately reproduced by using ultimately sophisticated functionals, for example, the CCSDT-level functionals of *ab initio* DFT[26] and the CCSD(T)-level potentials of the constrained-search method.[27] For unoccupied orbitals, orbital energies had never been provided even when using such sophisticated functionals. Surprisingly, long-range correction clearly solved this problem. Table 1 summarizes the mean absolute deviations of calculated highest occupied molecular orbital (HOMO) and lowest unoccupied molecular orbital (LUMO) energies from the minus of ionization potentials (IPs) and electron affinities (EAs), respectively.[28,29] As shown in the table, long-range correction drastically enhanced the reproducibility of orbital energies for both HOMOs and LUMOs and achieved in chemical accuracy. Since these errors were sufficiently small even when compared with the calculated IPs and EAs of the high-level *ab initio* CCSD(T) method, it was confirmed that long-range correction essentially solved the problem in orbital energy calculations. As far as we know, there is no other method giving quantitative HOMO and LUMO energies simultaneously. Therefore, the long-range corrected Kohn–Sham method is historically the first to provide quantitative orbital energies for both occupied and unoccupied orbitals. Note, however, that the HOMO energies of hydrogen and rare gas atoms are somewhat poor even when using long-range correction as mentioned later.

TABLE 1 | Mean Absolute Deviations in the Calculated Orbital Energies (eV) of Typical Molecules,[28] IP131 Benchmark Set,[29] and Hydrogen and Rare Gas Atoms[14]

Deviation	LC-BOP	B3LYP	BOP	HF
Typical molecules (20 molecules)				
ϵ_{HOMO} + IP	0.27	3.09	4.58	1.82
ϵ_{HOMO} + $IP_{CCSD(T)}$	0.21	3.13	4.89	0.77
ϵ_{LUMO} + EA	0.14	1.38	1.89	0.21
ϵ_{LUMO} + $EA_{CCSD(T)}$	0.21	1.80	2.33	0.44
IP131 benchmark set (113 molecules)				
ϵ_{HOMO} + IP	0.27	3.02	4.06	1.61
ϵ_{HOMO} + $IP_{CCSD(T)}$	0.32	3.09	4.54	0.85
ϵ_{LUMO} + EA	0.11	1.71	2.35	0.44
ϵ_{LUMO} + $EA_{CCSD(T)}$	0.24	2.06	2.46	0.62
H and rare gas atoms (5 atoms)				
ϵ_{HOMO} + IP	3.21	5.14	6.82	1.54
ϵ_{HOMO} + $IP_{CCSD(T)}$	2.88	4.81	6.51	0.79
ϵ_{LUMO} + EA	0.23	1.34	1.58	0.04
ϵ_{LUMO} + $EA_{CCSD(T)}$	0.81	2.05	2.21	0.57

So, why does long-range correction drastically improve orbital energies? To clarify the reason, it should be explained why HOMO and LUMO energies are identical to the corresponding minus ionization potentials and electron affinities, respectively. Although the HF method (with no SCF procedure) is well known to satisfy this identity on the basis of Koopmans' theorem,[30] many researchers seem not to recognize that this identity applies to the usual one-electron SCF methods. By combining Janak's theorem[31] and the energy linearity theorem for fractional occupations,[32,33] it is easily proved that every one-electron SCF method satisfies this relation. Janak's theorem establishes the relationship between total electronic energy and given orbital energy:

$$\frac{\partial E}{\partial n_i} = \epsilon_i, \tag{20}$$

where n_i is the occupation number of the ith orbital. That is, the total energy derivative with respect to the electron occupancy of an orbital is identical to the

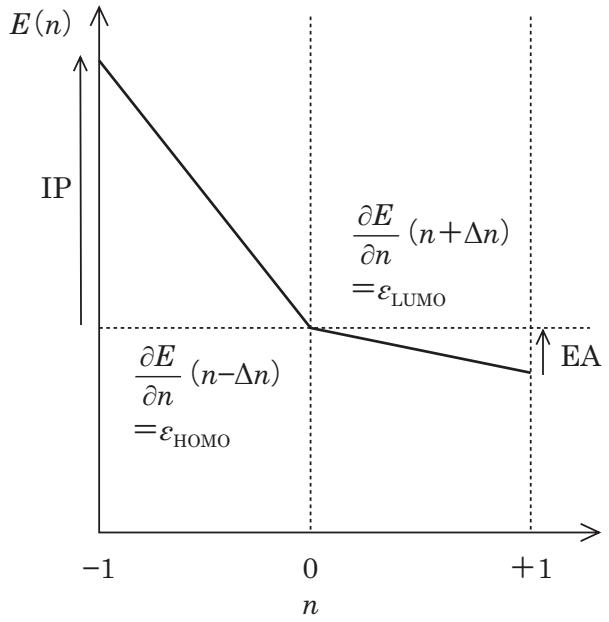

FIGURE 1 | Diagram of fractional occupation dependence of total electronic energy.

corresponding orbital energy. By fractional occupation calculations of total energies, it was confirmed that any one-electron SCF method satisfies Janak's theorem regardless of whether these are occupied or unoccupied orbitals. On the basis of the size-consistency and translational invariance of energy, a theorem was also proved to establish the linear dependence of total electronic energies on the fractional occupation,[32,33]

$$E\left(n+\frac{p}{q}\right)=\frac{p}{q}E(n+1)+\frac{q-p}{q}E(n). \qquad (21)$$

Combining this theorem with Janak's theorem clarifies the physical meaning of orbital energies. In Fig. 1, a diagram is illustrated for the total energy dependence on the fractional occupation number. The figure clearly shows that provided the total electronic energy satisfies the linearity theorem, Janak's theorem establishes that HOMO and LUMO energies are identical to the minus ionization potentials and electron affinities, respectively. Therefore, this combination is interpreted as a universal Koopmans' theorem for general one-electron SCF methods. Note that several studies have questioned the association of the LUMO energy with the minus electron affinity due to the possible discontinuity in the derivative of exchange-correlation functionals.[34,35] This question obviously comes from an unclear LUMO definition because the Koopmans' identity arises from Janak's and the energy linearity theorems similarly to the HOMO energy by reasonably defining the LUMO as the HOMO of monovalent anion. Combining Janak's and the energy linearity theorems also leads to a significant theorem for orbital energies, namely that orbital energies remain unchanged for fractional occupation numbers:

$$\epsilon_{n+1}(n+1)-\epsilon_{n+1}(n)=0. \qquad (22)$$

As easily checked, this theorem is proved by the invariance of the total electronic energy gradient for each occupation number of orbitals and the identity of the gradient and orbital energy. Note that Sham and Schlüter first suggested this theorem by assuming that the number of electrons, n, is large as seen in solid states, that is $\epsilon_{n+1}(n+1)-\epsilon_{n+1}(n)=O(n^{-1})\to 0$,[36] although this constant orbital energy theorem is also proved without this assumption by combining the Janak's and energy linearity theorems.

It was numerically confirmed that the Kohn–Sham method with long-range corrected functionals reproduces both the total electronic energy linearity and constant orbital energy theorems.[28] In Fig. 2, the calculated total electronic energies are illustrated in terms of the fractional occupation number. This figure clearly shows that only the long-range corrected functional provides the linearly varied total electronic energy irrespective of an increasing or decreasing number of electrons in the Kohn–Sham calculations. In contrast, other functionals give concave behavior of total electronic energies. Figure 3 plots the calculated orbital energies in terms of the fractional occupation number. As shown in the figure, the long-range corrected functional provides slightly decreasing but almost constant orbital energy in the Kohn–Sham calculation, whereas other functionals give considerably increasing orbital energies. Since the above results were obtained for almost all molecules, it was concluded that long-range correction enables the Kohn–Sham method to calculate accurate orbital energies for the first time.

Considering the dependence of orbital energies on the occupation number reveals the reason long-range correction makes it possible to give orbital energies quantitatively in the Kohn–Sham calculations. It was confirmed that assuming the occupation number independence of orbitals, Kohn–Sham orbital energies have the following occupation number dependence[28]:

$$\frac{\delta\epsilon_i}{\delta n_i}=\iint d^3\mathbf{r}_1 d^3\mathbf{r}_2\phi_i^*(\mathbf{r}_1)\phi_i^*(\mathbf{r}_2)\times\left[\frac{1}{r_{12}}+f_{\mathrm{xc}}\right]\phi_i(\mathbf{r}_1)\phi_i(\mathbf{r}_2), \qquad (23)$$

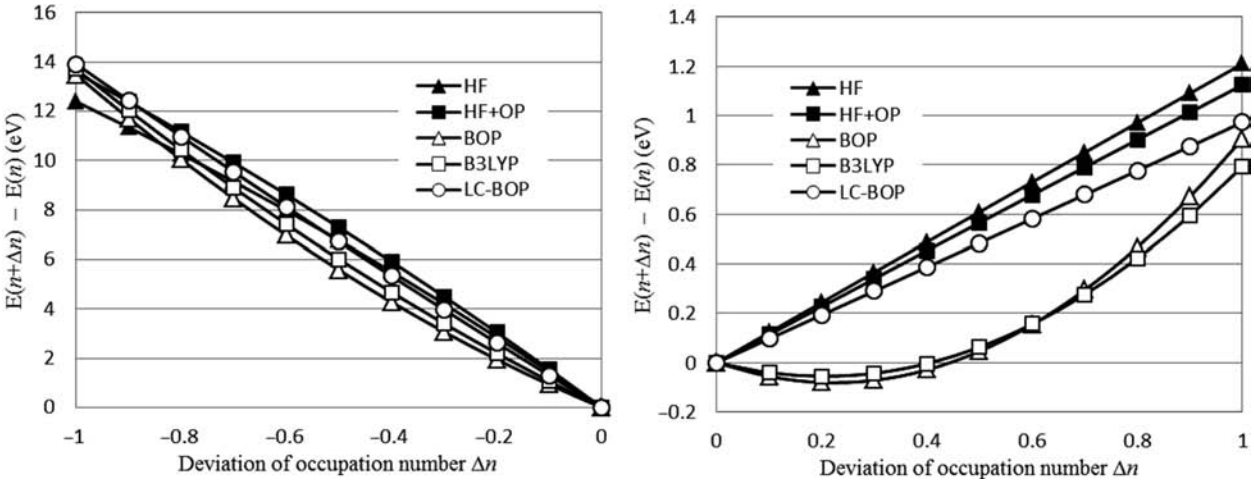

FIGURE 2 | Fractional occupation dependence of calculated total electronic energies of CO_2 molecule. Energies of neutral states are set to zero.

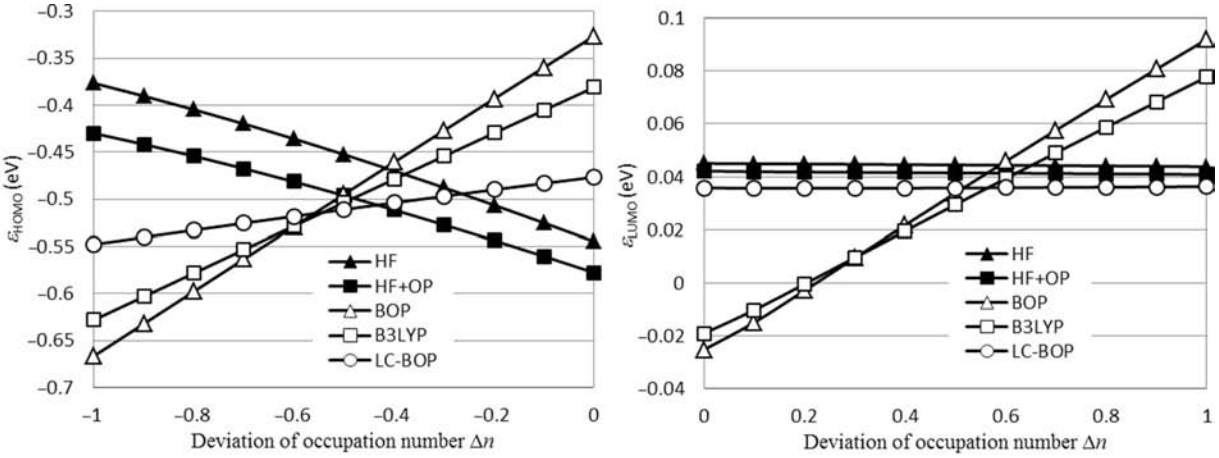

FIGURE 3 | Fractional occupation dependence of calculated orbital energies of CO_2 molecule.

where f_{xc} is the exchange-correlation integral kernel, $f_{xc} = \delta^2 E_{xc}/\delta\rho^2$. That is, the occupation number dependence of orbital energies is attributable to the self-interaction error of f_{xc}. Note that the contribution of the exchange-correlation integral kernel to the self-interactions arises almost completely from the exchange integral kernel unless considerable parallel-spin correlations are included, as seen in the LDA correlation functionals. For long-range corrected exchange functionals, the occupation number dependence of the calculated orbital energies is restricted to the short-range exchange part:

$$\frac{\delta\epsilon_i^{\mathrm{LC}}}{\delta n_i} = \iint d^3\mathbf{r}_1 d^3\mathbf{r}_2 \phi_i^*(\mathbf{r}_1)\phi_i^*(\mathbf{r}_2) \times \left[\frac{1-\mathrm{erf}\,(\mu r_{12})}{r_{12}} + f_{\mathrm{xc}}^{\mathrm{LC(sr)}}\right]\phi_i(\mathbf{r}_1)\phi_i(\mathbf{r}_2). \quad (24)$$

Actual calculations of atoms and molecules show that the long-range exchange part is dominant in the self-interactions through the exchange integral kernel except for rare gas atoms.[28] This indicates that the self-interaction errors in the exchange integral kernel are generally small for long-range corrected functionals, while they are obviously large without long-range correction. Therefore, long-range correction decreases the occupation number dependence of Kohn–Sham orbital energies to enhance the reproducibility of orbital energies.

Although long-range correction enables the Kohn–Sham method to calculate accurate valence orbital energies, it was reported that the HOMO energies of hydrogen and rare gas atoms are poorly given even when using long-range corrected functionals.[28] Similar errors are also found in the calculations of core orbital energies. Recently, one of us and a co-worker suggested that the LC-PR functional in

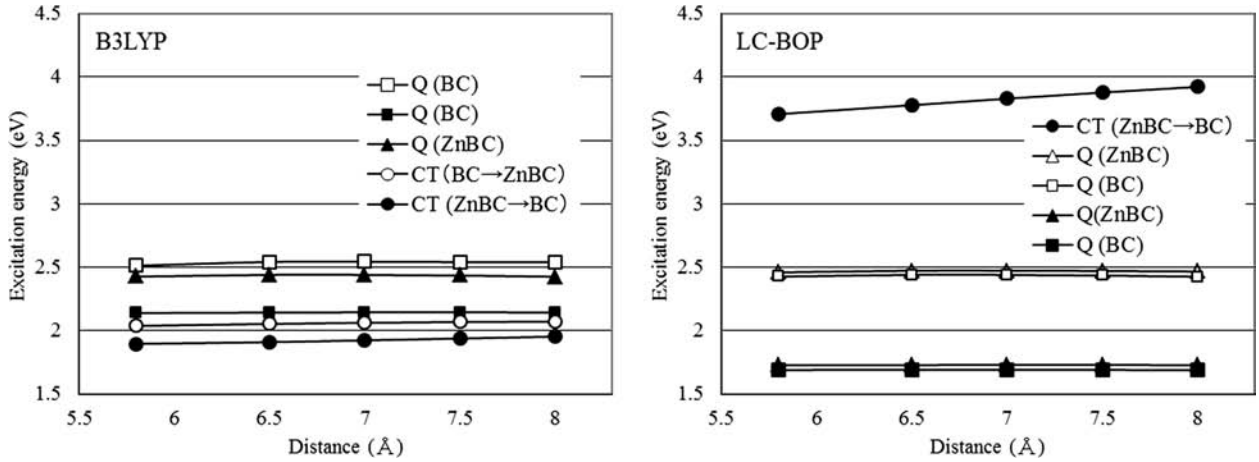

FIGURE 4 | Calculated excitation energies of Zn-bacteriochlorin-bacteriochlorin in terms of distance between centers of bacteriochlorins.

Eqs. (13) and (14) clearly solves this problem[14]: It drastically improves either the HOMO energies of hydrogen and rare gas atoms or core orbital energies, while maintaining or enhancing the accuracies in valence orbital energies. This indicates that the self-interaction error in the short-range exchange part also causes poor orbital energies.

Electron Excitation Spectra

Long-range correction provides a substantial improvement in electron excitation spectra. For many years, it has been reported that TDKS calculations significantly underestimate charge transfer[37,38] and Rydberg[39] excitation energies and oscillator strengths.[40] We and our co-workers have clearly shown that long-range correction solves all these underestimations.[41] Figure 4 illustrates the lowest excitation energies of Zn-bacteriochlorin-bacteriochlorin. Although experiments have shown that valence Q bands are the lowest excitations of this system, the TDKS calculations that use conventional functionals have provided charge transfer excitations lower than the Q bands.[38] As clearly shown in Fig. 4, a charge transfer excitation is obviously given above the Q bands, provided a long-range corrected functional is used. This indicates that the lack of long-range exchange interactions causes this problem. Besides, long-range correction clearly solves the problem in the charge transfer excitation energy of tetrafluoroethylene–ethylene dimer,[41] for which the dependence on the distance between molecules has been seriously underestimated when using conventional functionals.[37] Long-range correction is now established as the best strategy for reproducing charge transfer excitations in TDKS calculations. So far, long-range corrected TDKS studies have figured out various unknown mechanisms: for example, the initial process of TiO_2 photocatalytic reactions[42] and the photoinduced phase transition of tetrathiafulvalene-*p*-chloranil.[43] Furthermore, the excited-state geometry optimization based on the long-range corrected TDKS method[44] is now available in major quantum chemistry programs such as Gaussian 09[45] and has revealed the dual fluorescence mechanism of dimethylaminobenzonitrile[46] and anharmonic frequencies of excited states.[47] We, therefore, believe that the long-range corrected TDKS method is a core approach for investigating photochemical reactions quantitatively.

In the long-range corrected TDKS method, excitation energies are calculated by solving the matrix equation,[48]

$$(\mathbf{A}-\mathbf{B})^{1/2}(\mathbf{A}+\mathbf{B})(\mathbf{A}-\mathbf{B})^{1/2}\mathbf{F}_I = \omega_I^2 \mathbf{F}_I, \tag{25}$$

where ω_I is the Ith excitation energy and $\mathbf{F}_I$ is the corresponding response function. The elements of the matrices **A** and **B** are

$$A_{ia\sigma,jb\tau} = \delta_{ij}\delta_{ab}\delta_{\sigma\tau}(\epsilon_{a\sigma}-\epsilon_{i\sigma}) + K^{\mathrm{LC}}_{ia\sigma,jb\tau}, \tag{26}$$

and

$$B_{ia\sigma,jb\tau} = K^{\mathrm{LC}}_{ia\sigma,bj\tau}, \tag{27}$$

where $\epsilon_{i\sigma}$ is the ith σ-spin orbital energy. $K^{\mathrm{LC}}_{ia\sigma,jb\tau}$ is given by

$$K^{\mathrm{LC}}_{ia\sigma,jb\tau} = (ia\sigma|jb\tau) + \iint d^3\mathbf{r}_1 d^3\mathbf{r}_2 \phi^*_{i\sigma}(\mathbf{r}_1)\phi_{a\sigma}(\mathbf{r}_1) \times f_{\mathrm{xc}}^{\mathrm{LC(sr)}}(\mathbf{r}_1,\mathbf{r}_2)\phi_{j\tau}(\mathbf{r}_2)\phi^*_{b\tau}(\mathbf{r}_2) + K^{\mathrm{LC(lr)}}_{ia\sigma,jb\tau}, \tag{28}$$

where $f_{xc}(\mathbf{r}_1, \mathbf{r}_2)^{LC(sr)}$ is the long-range corrected exchange-correlation integral kernel,

$$f_{xc}^{LC(sr)}(\mathbf{r}_1, \mathbf{r}_2) = \frac{\delta^2\left[E_x^{LC(sr)} + E_c\right]}{\delta\rho_\sigma(\mathbf{r}_1)\delta\rho_\tau(\mathbf{r}_2)}. \quad (29)$$

In Eq. (28), the first term of the right-hand side is the Hartree integral,

$$(ia\sigma|jb\tau) = \iint d^3\mathbf{r}_1 d^3\mathbf{r}_2 \phi_{i\sigma}^*(\mathbf{r}_1)\phi_{a\sigma}(\mathbf{r}_1) \times \frac{1}{r_{12}}\phi_{j\tau}(\mathbf{r}_2)\phi_{b\tau}^*(\mathbf{r}_2), \quad (30)$$

and $K_{ia\sigma,bj\tau}^{LC(lr)}$ is the long-range exchange term,

$$K_{ia\sigma,jb\tau}^{LC(lr)} = -\delta_{\sigma\tau}\iint d^3\mathbf{r}_1 d^3\mathbf{r}_2 \phi_{j\sigma}^*(\mathbf{r}_1)\phi_{a\sigma}^*(\mathbf{r}_2) \times \frac{\mathrm{erf}(\mu r_{12})}{r_{12}}\phi_{i\tau}(\mathbf{r}_1)\phi_{b\tau}(\mathbf{r}_2). \quad (31)$$

Unless all $K_{ia\sigma,jb\tau}^{LC}$ terms are close to zero, excitation energies cannot be approximated by the corresponding orbital energy gaps.

The long-range corrected TDKS equation includes orbital energy gaps in the **A** matrix as shown in Eq. (26). Moreover, this equation uses the $\mathbf{K}^{LC}$ matrix, which contains the integrals of the exchange-correlation integral kernel in Eq. (28). In the preceding section, we described that only long-range corrected functionals accurately reproduce orbital energies and self-interactions through the exchange-correlation integral kernel. It was actually confirmed that both orbital energy gaps and exchange-correlation integral kernels are significantly underestimated in the Kohn–Sham calculations without long-range correction. Note, however, that plausible excitation energies are often obtained even without long-range correction due to the error cancellation of positive orbital energy gaps and negative exchange integral kernels. The most prominent example is valence excitations of small molecules, for which accurate excitation energies are obtained due to the similar shapes of orbitals before and after excitations. In contrast, for charge transfer and Rydberg excitations, the orbital shapes differ considerably before and after excitations to give a negligible **K** matrix. The underestimation of orbital energy gaps consequently causes severe errors in calculated excitation energies.

Response Properties

Similar to the electronic excitation spectra, serious problems have also been found in the calculations of response properties, which includes spectroscopic constants. It was reported that the optical response properties, for example, dipole moment, polarizability, and hyperpolarizability of long-chain polyenes, diverge in the coupled-perturbed Kohn–Sham and finite-field methods, provided conventional functionals are used.[49] We and our co-workers revealed that long-range correction clearly solves the overestimation of these response properties.[50] Figure 5 displays the calculated longitudinal hyperpolarizability of α,ω-nitro,amino-polyacetylene per unit with respect to the number of the units.[50] As clearly shown in the figure, the long-range corrected functional gives a plateau hyperpolarizability, which is close to that of the CCSD method, as the number of units increases, although conventional GGA and hybrid GGA functionals provide divergent hyperpolarizabilities. Similar behaviors are also found in the calculations of dipole moments and longitudinal polarizabilities. This indicates that the lack of long-range exchange interactions causes the divergent optical properties of long-chain polyenes. In addition, it was reported that long-range correction is quite efficient in hyperpolarizability calculations of diradicals. For the diradical character dependence of the hyperpolarizability of *p*-quinodimethane, it was found that only the long-range corrected functional presents an equivalent dependence to that of the highly accurate CCSD(T) method, whereas long-range uncorrected functionals give meaningless dependences.[51] Furthermore, in the second hyperpolarizability calculations of 1,4-bis-imidazol-2-ylidenecyclohexa-2,5-diene, which is known as a diradical, the long-range corrected functional is found to provide accurate values compared to the CCSD(T) results, in contrast to the results of long-range uncorrected functionals, which are inconsistent even for the signs. It is therefore concluded that long-range correction is one of the most powerful tools in Kohn–Sham-based response property calculations.

Response properties are essentially proportional to the energy derivatives in terms of various perturbations:[52]

$$\text{Response property} \propto \frac{\partial^{n_F+n_B+n_I+n_R}E}{\partial\mathbf{F}_{fld}^{n_F}\partial\mathbf{B}_{fld}^{n_B}\partial\mathbf{I}_{fld}^{n_I}\partial\mathbf{R}^{n_R}}, \quad (32)$$

where $\mathbf{F}_{fld}$, $\mathbf{B}_{fld}$, $\mathbf{I}_{fld}$, and $\mathbf{R}$ are the perturbations of the electric field, external magnetic field, internal magnetic field, and nuclear-coordinate vector, and n_X is the order of perturbation X. Therefore, energy derivatives should be calculated to obtain response properties, which include spectroscopic properties. Energy derivatives are represented as perturbation terms. Assuming the perturbed Kohn–Sham Hamiltonian

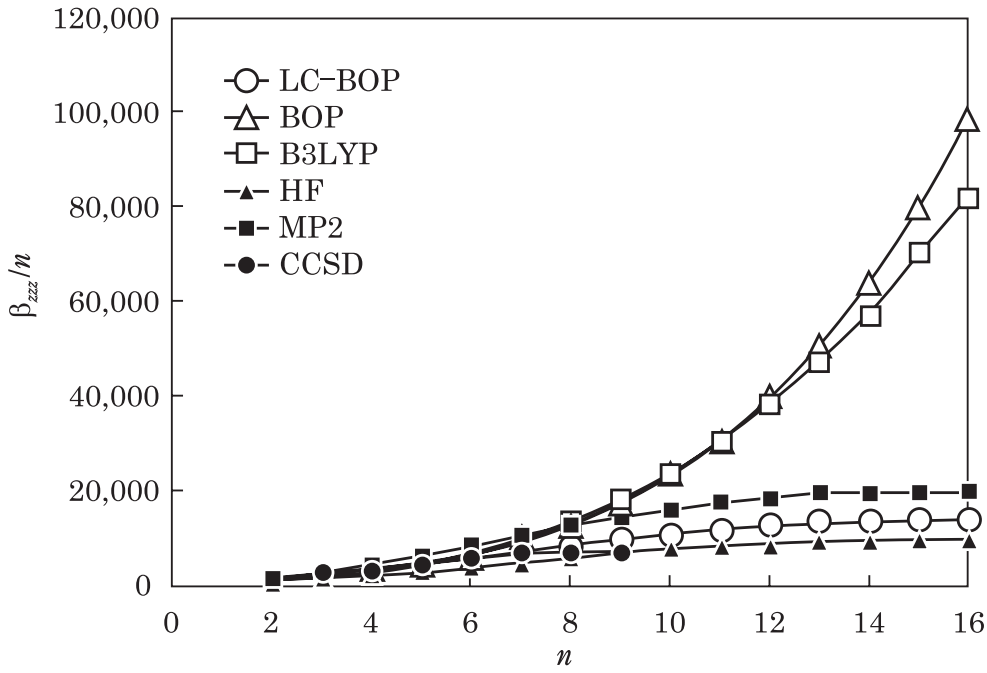

FIGURE 5 | Calculated longitudinal hyperpolarizabilities of α,ω-nitro,amino-polyacetylene per unit in terms of the number of units.

operator as

$$\hat{H} = \hat{H}_{\mathrm{KS}} + \lambda V_1 + \lambda^2 V_2, \tag{33}$$

where $\hat{H}_{\mathrm{KS}}$ is the Kohn–Sham Hamiltonian operator and V_n is the nth-order perturbation, the first and second energy derivatives are derived on the basis of the Rayleigh–Schrödinger perturbation theory[53] and the Hellmann–Feynman theorem[54] as

$$\left.\frac{\partial E_{\mathrm{KS}}}{\partial \lambda}\right|_{\lambda=0} = \langle \Psi_{\mathrm{KS}} | V_1 | \Psi_{\mathrm{KS}} \rangle , \tag{34}$$

where Ψ_{KS} is the Kohn–Sham wave function, and

$$\frac{1}{2}\left.\frac{\partial^2 E_{\mathrm{KS}}}{\partial \lambda^2}\right|_{\lambda=0} = \left\langle \frac{\partial \Psi_{\mathrm{KS}}}{\partial \lambda} \middle| V_1 \middle| \Psi_{\mathrm{KS}} \right\rangle + \left\langle \Psi_{\mathrm{KS}} \middle| V_2 \middle| \Psi_{\mathrm{KS}} \right\rangle, \tag{35}$$

respectively. In these equations, only the first derivative of the Kohn–Sham wave function in terms of a perturbation, $\partial\Psi_{\mathrm{KS}}/\partial\lambda$, is not available in advance to calculate the energy derivatives up to the second order. It was also proved that higher than third energy derivatives are also computable from wave function derivatives up to first order. Therefore, only the first wave function derivatives are required to calculate response properties.

Consideration of unitary transformation of orbitals makes it easy to solve for the first derivatives of orbitals. In the Kohn–Sham method, orbitals and orbital energies are obtained by diagonalizing the Fock matrix. Therefore, the nondiagonal terms of the Fock matrix are zero for orbitals, $\{\phi_i\}$,

$$F_{ia} = \int d^3\mathbf{r}\phi_i^*(\mathbf{r})\hat{F}_{\mathrm{KS}}\phi_a(\mathbf{r}) = h_{ia} + \sum_j^{n_{\mathrm{orb}}} \langle ij|aj\rangle + \int d^3\mathbf{r}\phi_i^*(\mathbf{r})V_{\mathrm{xc}}\phi_a(\mathbf{r}) = 0. \tag{36}$$

Since the Kohn–Sham wave function is a single Slater determinant, its derivative is given by the orbital variations, which are unitary-transformed under perturbation as

$$\phi_i' = \sum_j^{n_{\mathrm{basis}}} U'_{ji}\phi_j. \tag{37}$$

Substituting Eq. (37) into the first derivative of Eq. (36) leads to the coupled-perturbed Kohn-Sham equation,

$$\mathbf{AU}' = \mathbf{F}', \tag{38}$$

where matrix **A** is the same as that in Eq. (26), while neglecting spins. Although this equation is analogous to the time-dependent Kohn–Sham equation in Eq. (25), it should be noted that matrix **B** is neglected in Eq. (38) as usual to decrease the computational time by avoiding the difficulty in solving the equation. In Eq. (38), $\mathbf{F}'$ is the first derivative matrix of the Fock operator, which is usually derived as the first derivative of one-electron parts, h'_{ia}.[55] For the perturbation

of the uniform electric field, $\mathbf{F}_{\mathrm{fld}} = -F_{\mathrm{fld}}\mathbf{r}$, this is given as the matrix containing[56]

$$F'_{ia} = h'_{ia} = \frac{\partial h_{ia}}{\partial F_{\mathrm{fld}}} = -\int d^3\mathbf{r}\phi_i^*(\mathbf{r})\mathbf{r}\phi_a(\mathbf{r}). \qquad (39)$$

Using Eqs. (38) and (39), matrix $\mathbf{U}'$ is calculated to give the response properties in terms of the uniform electric field: dipole moment, polarizability, hyperpolarizability, and so forth. Other response properties are calculated by solving Eq. (38) after setting the first derivative of the Fock operator, $\mathbf{F}'$, in terms of each perturbation.

So, why can only long-range corrected functionals provide accurate response properties comprehensively? It is well known that for the ground states of typical small molecules, accurate response properties are reproduced even when using long-range uncorrected functionals. Similarly to the excitation energy calculations mentioned in the preceding section, it is also supposed to be due to the error cancellation. The errors in the orbital energy gaps in Eq. (26) and the exchange integral terms in Eq. (28) are usually cancelled out in the case that the electron distributions of orbitals are close to each other, as those in typical small molecules are. However, since the exchange integral terms are quite small for combinations of orbitals having much different electron distributions, the errors in the orbital energy gaps appear as the errors in the response properties. For this reason, it is supposed that long-range correction is required to give accurate response properties comprehensively.

Van der Waals Bonds

Long-range correction also drastically improves the poor Kohn–Sham results for van der Waals bonds. Since these bonds determine mainly the three-dimensional structures of large molecules, various methods have been developed to calculate them with both high accuracy and short computational time. For van der Waals calculations, there are many DFT-based methods, which focus mostly on reproducing accurate dispersion interactions. We and our coworkers showed for the first time that long-range exchange interactions are required to give accurate van der Waals bonds[57] and that the combination of a long-range corrected functional with a van der Waals term, which is called the "LC+vdW" method, is one of the best strategies for approaching this subject.[57] Although van der Waals interactions consist of ion–dipole, ion–induced dipole, dipole–dipole, dipole–induced dipole, and dispersion interactions, only the dispersion interactions are not incorporated in the Kohn–Sham method when using conventional functionals. Figure 6 illustrates the calculated dissociation potential curves of Ar dimer, in which the binding is formed only of dispersion interactions, for using various exchange functionals. As shown in the figure, although the dissociation potential curves of the dispersion significantly depend on the types of exchange functionals, this dependence disappears mostly after the long-range correction. This indicates that the repulsion of long-range exchange interactions plays a major role that balances with the attraction of dispersion interactions. In

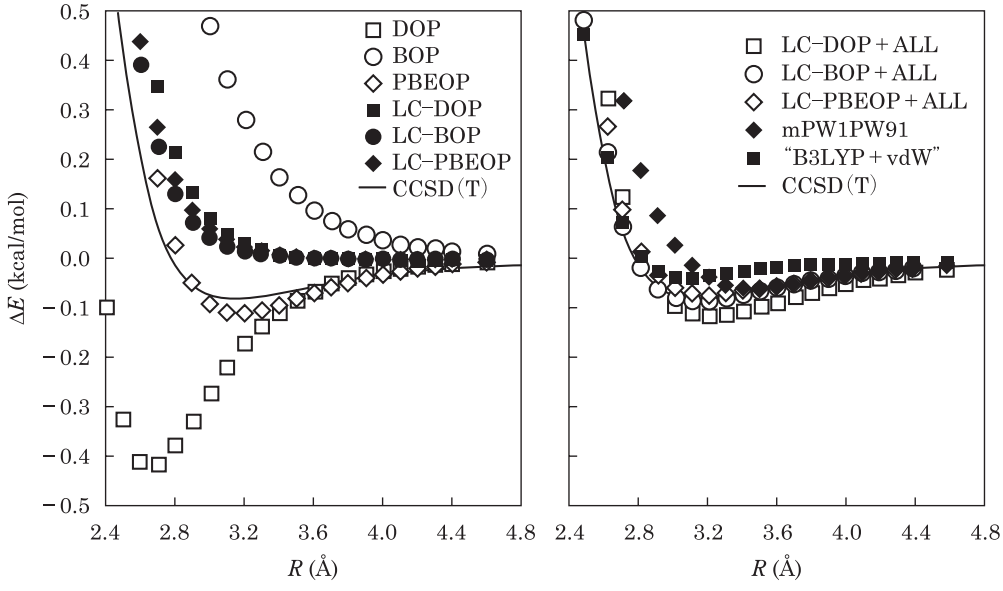

FIGURE 6 | Calculated potential energy curves of Ar dimer in terms of bond distance in kcal/mol.

another of our studies,[58] it was also revealed that long-range exchange interactions also determine dispersion bond angles. Figure 6 also shows that the types of correlation functionals considerably affect the dissociation potentials. This is because the LYP correlation functional overestimates correlation energies in the case of low density due to the violation of the high-density-gradient-low-density limit condition,[59]

$$\lim_{x_\sigma \to \infty} \rho^{-1} \bar{E}_c = 0, \tag{40}$$

where $\bar{E}_c$ is the integral kernel of a correlation functional. So far, we have applied this LC+vdW method to various weakly bonded systems and found that this method provides highly accurate binding energies for van der Waals and weak hydrogen bonds comprehensively.[58,60,61] We therefore suggest that both long-range correction and a correlation functional satisfying the high-density-gradient-low-density limit condition may be required in Kohn–Sham calculations of weakly bonded systems.

In the LC+vdW method, long-range corrected functionals are simply combined with van der Waals calculation methods to provide highly accurate van der Waals bonds. This is based on the fact that no dispersion interaction is contained in usual long-range corrected functionals, provided an appropriate correlation functional is used. In this case, the appropriate correlation functional has no dispersion interaction and satisfies Eq. (40), such as the one-parameter progressive (OP) correlation functional.[62] So far, the LC+vdW method has been combined with various van der Waals calculation methods. The combined calculation methods are classified into four types: semiempirical dispersion corrections, perturbation theories, the adiabatic connection/fluctuation-dissipation theorem (AC/FDT) method, and van der Waals functionals. In the semiempirical dispersion corrections, long-range corrected functionals are combined with the classical dispersion corrections multiplied by a semiempirical parameter. London's classical interatomic dispersion energy is usually used as the classical dispersion correction,

$$E^{\mathrm{LC+classical}} = E_{xc}^{\mathrm{LC}} - s_6 \sum_{A>B} \frac{C_6^{AB}}{{R_{AB}}^6} f_{\mathrm{damp}}(R_{AB}), \tag{41}$$

where A and B are usually the labels of atoms, C_6^{AB} denotes parameterized interatomic dispersion coefficients, s_6 is a semiempirical parameter, and f_{damp} is a damping function for cutting off unnecessary short-range interactions. An LC+vdW method combined with the semiempirical dispersion correction is "ωB97X-D" functional,[63] in which the parameterized classical dispersion correction is added to a long-range corrected functional, "ωB97X." In calculations on the S22 benchmark set that assembles 22 weakly bonded systems, this functional gives the most accurate binding energies among all van der Waals calculation methods for now, although this functional has a problem with including an enormous number of semiempirical parameters. An LC+vdW double hybrid method that incorporates electron correlation from second-order Møller–Plesset perturbation (MP2) theory[55] is[64,65]

$$E_{xc}^{\mathrm{LC+MP2}} = E_x^{\mathrm{LC}} + (1 - a_c)E_c + a_c E_c^{\mathrm{MP2}}. \tag{42}$$

Since the MP2 method reproduces dispersion interactions with relatively short computational time, these interactions can be incorporated in long-range corrected functionals by combining them with the MP2 correlation. An example of this method is the "ωB97X-2" functional,[66] which is also reported to give remarkably accurate results in the S22 benchmark set calculations. However, long-range dispersion correlations are not entirely included in this functional because the MP2 correlation is hybridized even for the long-range correlation. The applications may therefore be restricted to systems of intermediate size. Furthermore, there is an LC+vdW method combined with the long-range part of AC/FDT that is called "RPAx"[67]:

$$E_{xc}^{\mathrm{RSH+RPAx}} = E_{xc}^{\mathrm{RSH}} + E_c^{\mathrm{AC/FDT(lr)}}. \tag{43}$$

The AC/FDT method is a linear-response theory for calculating dispersion interactions on the basis of the Kohn–Sham method.[68] In this AC/FDT method, electron correlation is calculated as the energy response quantity for the spontaneous fluctuations of electronic motions coming from the perturbation of interelectronic interactions as

$$E_c^{\mathrm{AC/FDT}} = -\int_0^1 d\lambda \iint d^3\mathbf{r} d^3\mathbf{r}' \frac{1}{|\mathbf{r} - \mathbf{r}'|} \left[\frac{1}{2\pi} \int_0^\infty du \times \left\{ \chi_\lambda (\mathbf{r}, \mathbf{r}', iu) - \chi_0 (\mathbf{r}, \mathbf{r}', iu) \right\} \right], \tag{44}$$

where $\mathbf{r}$ and $\mathbf{r}'$ are the position vectors of electrons. In this equation, χ_λ and χ_0 are density response functions for interacting and independent electrons, respectively, and these are obtained by solving the Dyson equation as

$$\chi_\lambda (\mathbf{r}, \mathbf{r}', \omega) = \chi_0 (\mathbf{r}, \mathbf{r}', \omega) + \iint d^3\mathbf{r}_1 d^3\mathbf{r}_2 \chi_0 (\mathbf{r}, \mathbf{r}_1, \omega) \times \left\{ \frac{\lambda}{r_{12}} + f_{xc}^\lambda (\mathbf{r}_1, \mathbf{r}_2, \omega) \right\} \chi_\lambda (\mathbf{r}_2, \mathbf{r}', \omega), \tag{45}$$

TABLE 2 | Mean Absolute Deviations (MAD) of DFT Calculations Using Various Types of Dispersion Corrections for the S22 Benchmark Set in an Ascending Order (kcal/mol). The MAD of the MP2 Method at Complete Basis Set (CBS) Limit Is Also Displayed for Comparison

Method	Type of Correction(s)	MAD	Reference
ωB97X-D	LC + semiempirical	0.22	[63]
BLYP-D3	Semiempirical	0.23	[76]
ωB97X-2	LC + perturbation	0.26	[66]
LC-BOP+LRD	LC + vdW functional	0.27	[72]
B2PLYP-D3	Semiempirical + perturbation	0.29	[76]
RSH+RPAx-SO2	LC + AC/FDT	0.41	[77]
M06-2x	Semiempirical	0.44	[78]
BLYP-D	Semiempirical	0.55	[79]
B97-D	Semiempirical	0.61	[79]
B3LYP-D	Semiempirical	0.70	[79]
MP2/CBS	Perturbation	0.78	[76]
HF+VV09	vdW functional	0.89	[80]
M05-2x	semiempirical	0.90	[78]
vdW-DF(rPW86)	vdW functional	1.03	[80]
rPW86+VV09	vdW functional	1.20	[80]
vdW-DF(revPBE)	vdW functional	1.44	[80]
vdW-DF(HF)	vdW functional	2.80	[80]

where f_{xc}^{λ} is the exchange-correlation integral kernel for interacting systems. The electron correlation in Eq. (44) contains dispersion interactions as the long-range correlation. Analogously to the TDKS method, the correlation energy is calculated by solving the TDKS matrix equation. This AC/FDT method is obviously the most superior dispersion correction from a physical point of view. However, this method requires an enormous amount of computational time, which is more than a thousand times the time needed in Kohn–Sham calculations at present, unless drastic approximations are adopted. In the LC+vdW method,[57] the first combined van der Waals effect is a van der Waals functional, the Andersson–Langreth–Lundqvist (ALL) LDA dispersion functional[69]:

$$E_{xc}^{LC+ALL} = E_{xc}^{LC} - \frac{6}{4\pi^{3/2}} \int_{V_1} d^3\mathbf{r}_1 \int_{V_2} d^3\mathbf{r}_2 \times \frac{\sqrt{\rho(\mathbf{r}_1)}\sqrt{\rho(\mathbf{r}_1)}}{\sqrt{\rho(\mathbf{r}_1)} + \sqrt{\rho(\mathbf{r}_1)}} \frac{1}{r_{12}^6} f_{damp}(r_{12}). \quad (46)$$

This LC+ALL method has accurately reproduced various van der Waals and weak hydrogen bonds.[58,60,61] However, the ALL functional has a limitation in accuracy because it is an LDA functional. The local response dispersion (LRD) functional was developed to overcome this limitation. In this functional, the dispersion coefficient based on a local response approximation[70] is combined with a dielectric model for smoothing the real-space cutoff[71] to give a GGA dispersion functional. This LC+LRD method not only has the highest level of accuracy in the S22 benchmark set calculations[72] but has clearly solved or clearly improved various problems in the Kohn–Sham calculations: underestimated isodesmic reaction enthalpies,[73] underestimated branching reaction enthalpies,[74] and overestimated Diels–Alder reaction barriers.[75]

The LC+vdW method comes before other van der Waals calculation methods in terms of the accuracy of the calculated binding energies for the S22 benchmark set. As mentioned above, the S22 benchmark set, which assembles 22 weakly bonded systems, is the most frequently used trial set for evaluating the reproducibility of van der Waals methods in the calculations of weak bonds such as van der Waals and weak hydrogen bonds. Table 2 arranges the mean absolute errors in the calculated binding energies of the S22 set with the names and correction types of the van der Waals calculation methods in an ascending order of errors. In the table, it is found that four of the top six highly accurate methods are LC+vdW methods. It is noteworthy that the LC+vdW methods overtake semiempirical functionals, in most of which semiempirical parameters are fitted to give accurate results for this S22 set, in terms of accuracy. Furthermore, since the vdW-DF method uses a GGA-level dispersion functional similarly to the LC+LRD method, the major difference in accuracy between these methods is attributable to the presence or absence of long-range correction. We, therefore, suppose that the

repulsion of long-range exchange interactions plays a major role in weak bonds such as van der Waals bonds, and, therefore, long-range correction is the best strategy for enhancing the accuracy of the Kohn–Sham method in the calculations of weakly bonded systems.

CONCLUSIONS

Long-range correction complements the long-range exchange effects in exchange density functionals by combining the short-range part of exchange functionals with the long-range part of the HF exchange integral. Despite its simple form that uses only one parameter, this correction has solved or drastically improved a wide variety of problems in Kohn–Sham density functional calculations. Because of its high applicability, various types of long-range corrected functionals have been developed: CAM-B3LYP, LC-ωPBE, ωB97X, LC-PR, and so forth. Major properties that the long-range correction has solved are valence orbital energies, electronic excitation spectra, response properties, and van der Waals bonds. Orbital energies, which are the solutions of the Kohn–Sham method, have been poorly calculated in the past, although occupied valence orbital energies have recently been given quantitatively by ultimately sophisticated methods. Surprisingly, the long-range corrected functionals reproduced valence occupied and unoccupied orbital energies quantitatively for the first time. This is because the long-range correction drastically decreases the self-interaction error of the exchange integral kernel, which is the derivative of the exchange potential in terms of density. In the calculations of electronic excitation spectra and response properties, conventional functionals have underestimated charge transfer and Rydberg excitation energies and oscillator strengths in TDKS calculations and have provided poor optical properties such as hyperpolarizabilities in CPKS and finite-field calculations. Long-range correction has clearly solved these problems by enhancing the accuracies in the orbital energy gaps and exchange integral kernels, which are used in these calculations. Furthermore, long-range correction also drastically improves the reproducibility of van der Waals bonds. The LC+vdW method, which simply combines a long-range corrected functional with a conventional van der Waals calculation method, occupied the top rank in calculations of the S22 benchmark set, which is the most frequently used trial set for evaluating the reproducibility of weakly bonded systems. Therefore, we conclude that long-range correction is essentially required in exchange functionals to investigate chemistries on the basis of the Kohn–Sham calculations.

ACKNOWLEDGMENTS

This research was supported by the Japanese Ministry of Education, Culture, Sports, Science and Technology (grant: 23225001 and 24350005).

REFERENCES

1. Iikura H, Tsuneda T, Yanai T, Hirao K. A long-range correction scheme for generalized-gradient-approximation exchange functionals. *J Chem Phys* 2001, 115:3540–3544.
2. Dirac PAM. Note on exchange phenomena in the Thomas atom. *Camb Phil Soc* 1930, 26:376–385.
3. Savin A. On degeneracy, near-degeneracy and density functional theory. In: Seminario JJ, ed. *Recent Developments and Applications of Modern Density Functional Theory*. Amsterdam: Elsevier; 1996, 327–357.
4. Song J-W, Hirosawa T, Tsuneda T, Hirao K. Long-range corrected density functional calculations of chemical reactions: Redetermination of parameter. *J Chem Phys* 2007, 126:154105.
5. Yanai T, Tew DP, Handy NC. A new hybrid exchange-correlation functional using the Coulomb-attenuating method (CAM-B3LYP). *Chem Phys Lett* 2004, 91:51–57.
6. Becke AD. Density-functional thermochemistry. III. The role of exact exchange. *J Chem Phys* 1993, 98:5648–5652.
7. Lee C, Yang W, Parr RG. Development of the Colle-Salvetti correlation-energy formula into a functional of the electron density. *Phys Rev B* 1988, 37:785–789.
8. Vydrov OA, Heyd J, Krukau A, Scuseria GE. Importance of short-range versus long-range Hartree-Fock exchange for the performance of hybrid density functionals. *J Chem Phys* 2006, 125:074106.

9. Ernzerhof M, Perdew JP. Generalized gradient approximation to the angle- and system-averaged exchange hole. *J Chem Phys* 1998, 109:3313–3320.
10. Chai J-D, Head-Gordon M. Long-range corrected hybrid density functionals with damped atom-atom dispersion corrections. *J Chem Phys* 2008, 128:084106.
11. Becke AD. Density-functional thermochemistry. V. Systematic optimization of exchange-correlation functionals. *J Chem Phys* 1997, 107:8554–8560.
12. Tao J, Perdew JP, Staroverov VN, Scuseria GE. Climbing the density functional ladder: nonempirical meta-generalized gradient approximation designed for molecules and solids. *Phys Rev Lett* 2003, 91: 146401.
13. Goll E, Ernst M, Moegle-Hofacker F, Stoll H. Development and assessment of a short-range meta-GGA functional. *J Chem Phys* 2009, 130:234112.
14. Nakata A, Tsuneda T. Density functional theory for comprehensive orbital energy calculations. *J Chem Phys* 2013, 139:064102.
15. Nakata A, Tsuneda T, Hirao K. Modified regional self-interaction correction method based on the pseudospectral method. *J Phys Chem A* 2010, 114:8521–8528.
16. Tsuneda T, Kamiya M, Hirao K. Regional self-interaction correction of density functional theory. *J Comput Chem* 2003, 24:1592–1598.
17. Orszag SA. Comparison of pseudospectral and spectral approximation. *Stud Appl Math* 1972, 51:253–259.
18. Toulouse J, Colonna F, Savin A. Long-range–short-range separation of the electron-electron interaction in density-functional theory. *Phys Rev A* 2004, 70:062505.
19. Toulouse J, Colonna F, Savin A. Short-range exchange and correlation energy density functionals: beyond the local-density approximation. *J Chem Phys* 2005, 122:0114110.
20. Song J-W, Tokura S, Sato T, Watson MA, Hirao K. An improved long-range corrected hybrid exchange-correlation functional including a short-range Gaussian attenuation (LCgau-BOP). *J Chem Phys* 2007, 127:154109.
21. Cohen AJ, Mori-Sanchez P, Yang W. Development of exchange-correlation functionals with minimal many-electron self-interaction error. *J Chem Phys* 2007, 126:191109.
22. Livshits E, Baer R. A well-tempered density functional theory of electrons in molecules. *Phys Chem Chem Phys* 2007, 9:2932–2941.
23. Peverati R, Truhlar DG. Improving the Accuracy of Hybrid Meta-GGA Density Functionals by Range Separation. *J Phys Chem Lett* 2011, 2:2810–2817.
24. Akinaga Y, Ten-no S. Intramolecular charge-transfer excitation energies from range-separated hybrid functionals using the Yukawa potential. *Int J Quantum Chem* 2009, 109:1905–1914.
25. Seth M, Ziegler T. Range-separated exchange functionals with Slater-type functions. *J Chem Theory Comput* 2012, 8:901–907.
26. Schweigert IV, Bartlett RJ. Effect of the nonlocal exchange on the performance of the orbital-dependent correlation functionals from second-order perturbation theory. *J Chem Phys* 2008, 129:124109.
27. Teale AM, De Proft F, Tozer DJ. Orbital energies and negative electron affinities from density functional theory: insight from the integer discontinuity. *J Chem Phys* 2008, 129:044110.
28. Tsuneda T, Song J-W, Suzuki S, Hirao K. On Koopmans' theorem in density functional theory. *J Chem Phys* 2010, 133:174101.
29. Kar R, Song J-W, Hirao K. Long-range corrected functionals satisfy Koopmans' theorem: calculation of correlation and relaxation energies. *J Comput Chem* 2013, 34:958–964.
30. Koopmans T. Über die zuordnung von wellenfunktionen und eigenwerten zu den einzelnen elektronen eines atoms. *Physica* 1934, 1:104–113.
31. Janak JF. Proof that ∂ E∂ ni = ε in density-functional theory. *Phys Rev B* 1978, 103:7165–7168.
32. Perdew JP, Parr RG, Levy M, Balduz JLJ. Density-functional theory for fractional particle number: derivative discontinuities of the energy. *Phys Rev Lett* 1982, 49:1691–1694.
33. Yang W, Zhang Y, Ayers PW. Degenerate ground states and a fractional number of electrons in density and reduced density matrix functional theory. *Phys Rev Lett* 2000, 84:5172–5175.
34. Kronik L, Stein T, Rafaely-Abramson S, Baer R. Excitation gaps of finite-sized systems from optimally tuned range-separated hybrid functionals. *J Chem Theory Comput* 2012, 8:1515–1531.
35. Cohen AJ, Mori-Sanchez P, Yang W. Challenges for density functional theory. *Chem Rev* 2012, 112:289–320.
36. Sham LJ, Schlüter M. Density-functional theory of the band gap. *Phys Rev B* 1985, 32:3883–3889.
37. Dreuw A, Weisman JL, Head-Gordon M. Long-range charge-transfer excited states in time-dependent density functional theory require non-local exchange. *J Chem Phys* 2003, 119:2943–2946.
38. Dreuw A, Head-Gordon M. Failure of time-dependent density functional theory for long-range charge-transfer excited states: the zincbacteriochlorin–bacteriochlorin and bacteriochlorophyll–spheroidene complexes. *J Am Chem Soc* 2004, 126:4007–4016.
39. Tozer DJ, Handy NC. Improving virtual Kohn-Sham orbitals and eigenvalues: application to excitation energies and static polarizabilities. *J Chem Phys* 1998, 109:10180–10189.
40. van Gisbergen SJA, Kootstra F, Schipper PRT, Gritsenko OV, Snijders JG, Baerends EJ. Density-functional-theory response-property calculations with

accurate exchange-correlation potentials. *Phys Rev A* 1998, 57:2556–2571.

41. Tawada Y, Tsuneda T, Yanagisawa S, Yanai T, Hirao K. A long-range-corrected time-dependent density functional theory. *J Chem Phys* 2004, 120:8425–8433.
42. Suzuki S, Tsuneda T, Hirao K. A theoretical investigation on photocatalytic oxidation on the TiO_2 surface. *J Chem Phys* 2012, 136:024706.
43. Nakatsuka T, and Tsuneda Y, Sato T, Hirao K. Theoretical Investigations on the Photoinduced Phase transition mechanism of etrathiafulvalene-p-chloranil. *J Chem Theor Comput* 2011, 7:2233–2239.
44. Chiba M, Tsuneda T, Hirao K. Excited state geometry optimizations by analytical energy gradient of long-range corrected time-dependent density functional theory. *J Chem Phys* 2006, 124:144106.
45. Frisch MJ, Trucks GW, Schlegel HB, Scuseria GE, Robb MA, Cheeseman JR, Scalmani G, Barone V, Mennucci B, Petersson GA, et al. *Gaussian 09 Revision A.1*, gaussian Inc., Wallingford CT 2009.
46. Chiba M, Tsuneda T, Hirao K. Long-range corrected time-dependent density functional study on fluorescence of 4, 4-dimethylaminobenzonitrile. *J Chem Phys* 2007, 126:034504.
47. Tokura S, Yagi K, Tsuneda T, Hirao K. Anharmonic vibrational state calculations in the electronic excited states studied by time-dependent density functional theory. *Chem Phys Lett* 2007, 436:30–35.
48. Casida ME. Time-dependent density functional response theory of molecular systems: theory, computational methods, and functionals. In: Seminario JJ ed. *Recent Developments and Applications of Modern Density Functional Theory*. Amsterdam: Elsevier; 1996, 391–439.
49. Champagne B, Perpéte EA, Jacquemin D. Assessment of conventional density functional schemes for computing the dipole moment and (hyper)polarizabilities of push–pull π-conjugated systems. *J Phys Chem A* 2000, 104:4755–4763.
50. Kamiya M, Sekino H, Tsuneda T, Hirao K. Nonlinear optical property calculations by the long-range-corrected coupled-perturbed Kohn-Sham method. *J Chem Phys* 2005, 122:234111.
51. Kishi R, Bonness S, Yoneda K, Takahashi H, Nakano M, Botek E, Champagne B, Kubo T, Kamada K, Ohta K, et al. Long-range corrected density functional theory study on static second hyperpolarizabilities of singlet diradical systems. *J Chem Phys* 2010, 132:094107.
52. Jensen F. *Introduction to Computational Chemistry*. Chichester: Wiley; 2006.
53. Schrödinger E. Quantisierung als eigenwertproblem. *Ann Phys* 1926, 80:437–439.
54. Feynman RP. Forces in molecules. *Phys Rev* 1939, 56:340–343.
55. McWeeny R. *Methods of Molecular Quantum Mechanics*. 2nd ed. San Dieg CA: Academic Press; 1992.
56. Lee AM, Colwell SM. The determination of hyperpolarizabilities using density functional theory with nonlocal functionals. *J Chem Phys* 1994, 101:9704.
57. Kamiya M, Tsuneda T, Hirao K. A density functional study of van der Waals interactions. *J Chem Phys* 2002, 117:6010–6015.
58. Sato T, Tsuneda T, Hirao K. A density-functional study on π-aromatic interaction: Benzene dimer and naphthalene dimer. *J Chem Phys* 2007, 126:234114.
59. Dreizler RM, Gross EKU. *Density-Functional Theory an Approach to the Quantum Many-Body Problem*. Berlin: Springer; 1990.
60. Sato T, Tsuneda T, Hirao K. A density-functional study on π-aromatic interaction: benzene dimer and naphthalene dimer. *J Chem Phys* 2005, 123:104307.
61. Sato T, Tsuneda T, Hirao K. Van der Waals interactions studied by density functional theory. *Mol Phys* 2005, 103:1151–1164.
62. Tsuneda T, Suzumura T, Hirao K. A new one-parameter progressive Colle-Salvetti-type correlation functional. *J Chem Phys* 1999, 110:10664–10678.
63. Chai J-D, Head-Gordon M. Long-range corrected hybrid density functionals with damped atom-atom dispersion corrections. *Phys Chem Chem Phys* 2008, 10:6615.
64. Angyan JG, Gerber IC, Savin A, Toulouse J. van der Waals forces in density functional theory: perturbational long-range electron-interaction corrections. *Phys Rev A* 2005, 72:012510.
65. Grimme S. Semiempirical hybrid density functional with perturbative second-order correlation. *J Chem Phys* 2006, 124:034108.
66. Chai J-D, Head-Gordon M. Long-range corrected double-hybrid density functionals. *J Chem Phys* 2009, 131:174105.
67. Zhu W, Toulouse J, Savin A, Angyan JG. Range-separated density-functional theory with random phase approximation applied to noncovalent intermolecular interactions. *J Chem Phys* 2010, 132:244108.
68. Langreth DC, Perdew JP. The exchange-correlation energy of a metallic surface. *Solid State Commun* 1975, 17:1425–1429.
69. Andersson Y, Langreth DC, Lundqvist BI. van der Waals interactions in density-functional theory. *Phys Rev Lett* 1996, 76:102–105.
70. Dobson JF, Dinte BP. Constraint satisfaction in local and gradient susceptibility approximations: application to a van der Waals density functional. *Phys Rev Lett* 1996, 76:1780–1783.
71. Vydrov OA, van Voorhis T. Improving the accuracy of the nonlocal van der Waals density functional with minimal empiricism. *J Chem Phys* 2009, 130:104105.

72. Sato T, Nakai H. Density functional method including weak interactions: dispersion coefficients based on the local response approximation. *J Chem Phys* 2009, 131:224104.
73. Song J-W, Tsuneda T, Sato T, Hirao K. Calculations of alkane energies using long-range corrected DFT combined with Intramolecular van der Waals correlation. *Org Lett* 2010, 12:1440–1443.
74. Song J-W, Tsuneda T, Sato T, Hirao K. An examination of density functional theories on isomerization energy calculations of organic molecules. *Theor Chem Acc* 2011, 130:851–857.
75. Singh RK, Tsuneda T. Reaction energetics on long-range corrected density functional theory: Diels-Alder reactions. *J Comput Chem* 2013, 34:379–386.
76. Grimme S, Antony J, Ehrlich S, Krieg H. A consistent and accurate ab initio parametrization of density functional dispersion correction (DFT-D) for the 94 elements H-Pu. *J Chem Phys* 2010, 132:154104.
77. Toulouse J, Zhu W, Savin A, Jansen G, Angyan JG. Closed-shell ring coupled cluster doubles theory with range separation applied on weak intermolecular interactions. *J Chem Phys* 2011, 135:084119.
78. Pernal K, Podeszwa R, Patkowski K, Szalewicz K. Dispersionless density functional theory. *Phys Rev Lett* 2009, 103:263201.
79. Antony J, Grimme S. Density functional theory including dispersion corrections for intermolecular interactions in a large benchmark set of biologically relevant molecules. *Phys Chem Chem Phys* 2006, 8:5287–5293.
80. Vydrov OA, VanVoorhis T. Nonlocal van der Waals density functional: the simpler the better. *J Chem Phys* 2010, 132:164113.

